Proceedings of the 39th IAHR World Congress
19-24 June
2022 Granada, Spain
DOI
number

A Two-Layer Model for the Numerical Simulation of Oil Spills over Coastal Flows

Isabel Echeverribar[(1)], Pilar Brufau[(2)] and Pilar García-Navarro[(3)]

[(1,2,3)] Fluid Mechanics, I3A-University of Zaragoza, Zaragoza, Spain
e-mail echeverribar@unizar.es
[(1)] Hydronia Europe, Madrid, Spain,

Abstract

Nowadays, the vast majority of models for oil spill simulation are based on Lagrangian methods focused on particle tracking algorithms to represent the oil slick. In this work, an Eulerian model for the simulation of oil spills over water is implemented by means of a particular two-layer shallow water model based on a finite volume upwind scheme with a Roe solver for both oil slick and water column. By assuming a very thin layer of oil floating and being transported over a huge volume of water, the pressure term that the upper layer exerts over the lower layer can be neglected. However, friction terms between layers are considered so that the oil flows over a movable water volume being transported by friction stresses. The main advantage of this model is the capability of solving the evolution of the oil layer, computing the oil depth and the velocity field. Special emphasis is placed on the treatment of the two-layer wet-dry boundary, as the aim of the model is to compute the front spreading of oil slicks. Additionally, the two-layer model allows the simulation of the oil spill flowing overland once the bare terrain is reached -as in coastal spills might occur- by changing the friction law. Preliminar results in 1D cases are presented

Keywords: *two-layer; numerical simulation; shallow water; non-hydrostatic pressure; oil-spill*

1. INTRODUCTION

When an oil spill occurs over a water body, several mechanisms act to spread the oil slick over the surface, before other fate processes start. The final extension of oil spills can be estimated empirically by analyzing separately the four acting forces: gravity, inertia, viscous stress and surface tension (Hoult 1972). Earlier works have focused on the development of empirical laws to get an idea of the maximum extension of an oil slick, but usually need a previous estimation of the distribution of some variables, such as the oil slick thickness, is requiered. More complex models to carry out estimations based on some kinematic simplified equations that need to be numerically solved have also been proposed (Hoult 1972). In any case, all those models were far from being a complete integrated model.

The development of efficient numerical methods improved oil spills simulation. The vast majority of models are based on Lagrangian methods focused on particle tracking algorithms to represent the oil slick (Spaulding 2017) while solving the water dynamics with Eulerian models; although there also exist some Eulerian models to solve the oil slick thickness and dynamics. They usually take the water column velocity field as an input (Tkalich, 2006) and focus only the computation on the oil slick and its properties.

In this work, a complete model for the simulation of oil spills over water is implemented by means of a particular two-layer shallow water model. The mass and momentum conservation equations are formulated to model the two-layers, which are coupled through the source terms. Other two-layer models contain friction source terms between layers, as well as pressure terms, to provide the coupling mechanism (Martínez-Aranda *et al.* 2020; Murillo *et al.* 2020). The lower layer acts as the unsteady bottom of the upper layer affecting its dynamics. Additionally, the upper layer might exert a pressure over the lower layer due to its weight. In the present model, oriented to be applied to thin layers of oil spills over huge water volumes, this term is neglected for dimensional reasons, avoiding some numerical difficulties previously reported (Martínez-Aranda *et al.* 2020).

A one-dimensional (1D) finite volume upwind scheme with a Roe solver is used to discretize the computational domain and carry out the simulation, solving both oil slick and water column. By assuming a very thin layer of oil floating and being transported over a huge volume of water, the pressure term that the upper layer exerts over the lower layer can be neglected. However, friction terms between layers are considered so that the oil flows over a movable water volume being transported by friction stresses. The main advantage of this model is the capability of solving the evolution of the oil layer, computing the oil depth and

the velocity field. Special emphasis is placed on the treatment of the two-layer wet-dry mechanisms following Murillo (2013), as the aim of the model is to compute the front spreading of oil slicks. Additionally, the two-layer model allows the simulation of the oil spill flowing overland once the bare terrain is reached -as in coastal spills might occur- by changing the friction law, that turns into a Manning law instead of Chézy interface friction law.

Finally, in order to simulate the horizontal temperature gradients, a transport equation derived from the conservation of internal energy has been added to the upper layer to represent the temperature transport in the upper layer. The simulation of temperature in water masses is commonly performed as the passive transport of a scalar (Dugdale *et al.* 2017). However, in this model it is intended as a preliminary step before an extension to more complex models where the temperature has a presence in the momentum equations (Ripa 1995).

2. TWO-LAYER MODEL WITH TEMPERATURE TRANSPORT

This section describes the chosen system of equations and the 1D numerical scheme implemented to solve the system. As depicted in Figure 1, all the variables with suffix 1 correspond to the upper layer, while the lower layer is denoted with suffix 2.

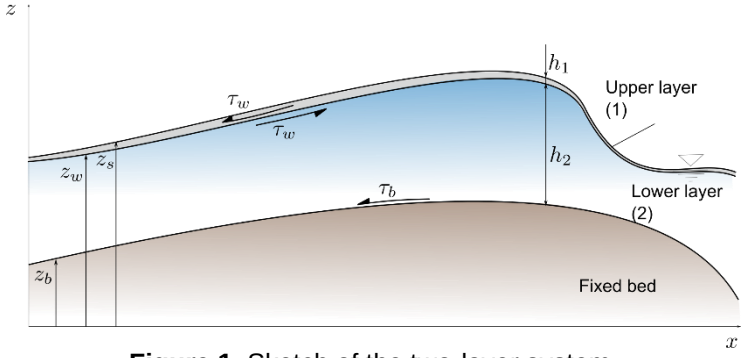

Figure 1. Sketch of the two-layer system.

2.1 System of equations

For each of the layers, the depth averaged mass and x-momentum conservation are written with the pertinent source terms of bottom and friction

$$\frac{\partial(h_1)}{\partial t}+\frac{\partial(h_1u_1)}{\partial x}=0 \quad [1]$$

$$\frac{\partial(h_1u_1)}{\partial t}+\frac{\partial}{\partial x}\left(h_1u_1^2+\frac{1}{2}gh_1^2\right)=-gh_1\frac{\partial z_b}{\partial x}-gh_1\frac{\partial h_2}{\partial x}-\frac{\tau_w}{\rho_1} \quad [2]$$

$$\frac{\partial(h_2)}{\partial t}+\frac{\partial(h_2u_2)}{\partial x}=0 \quad [3]$$

$$\frac{\partial(h_2u_2)}{\partial t}+\frac{\partial}{\partial x}\left(h_2u_2^2+\frac{1}{2}gh_2^2\right)=-gh_2\frac{\partial z_b}{\partial x}-\frac{\tau_b}{\rho_2}-\frac{\tau_w}{\rho_2} \quad [4]$$

where τ_b stands for the stress due to friction stresses with bottom, at z_b, and τ_w represents the friction between the layers, at z_w (see Figure 1). Friction between terrain and the lower layer is modelled with a turbulent Manning law, while friction between layers follows a Chezy formula as

$$\tau_b = \rho_2 g h_2 C_b u_2|u_2| \; with \; C_b = \frac{n_b^2}{h_2} \quad [5]$$

$$\tau_w = \rho_1 g C_{fw,1}(u_1-u_2)|u_1-u_2| = \rho_2 g C_{fw,2}(u_1-u_2)|u_1-u_2| \quad [6]$$

being n_b the Manning coefficient and C_{fw} a Chézy-type friction coefficient that represents the interface friction, related with densities as $C_{fw,2} = rC_{fw,1}$, where r stands for density relation as $r = \rho_1/\rho_2$.

Additionally, the temperature of the upper layer (layer 1) is transported as a passive scalar with an equation derived by the internal energy conservation equation as

$$\frac{\partial (hT)_1}{\partial t} + \frac{\partial (huT)_1}{\partial x} = -K_d \frac{\partial^2 T_1}{\partial x^2} + \frac{\dot{Q}_{TOT}}{\rho_1 C_p} \quad [7]$$

where the diffusion term, through a diffusion coefficient K_d, is neglected in order to focus on the convective terms, C_p stands for the specific heat [J/(kg·K)] and $\dot{Q}_{TOT}$ represents the total rate of heat exchange per unit surface area [W/m^2].

2.2 **Numerical scheme**

A first order explicit finite volume numerical method is used to solve the dynamics of the system (1)-(7). A Roe type Riemann solver is applied at cell edges to compute contributions following Murillo and García-Navarro (2013). This kind of schemes, which have been validated as robust, stable and steady state preserving, follow an updated scheme for each cell at each time as:

$$\mathbf{U}_i^{n+1} = \mathbf{U}_i^n - \frac{\Delta t}{\Delta x}\left[\left(\tilde{\lambda}^+ \tilde{\gamma} \tilde{\mathbf{e}}\right)_{i-1/2} + \left(\tilde{\lambda}^- \tilde{\gamma} \tilde{\mathbf{e}}\right)_{i+1/2}\right]^n \quad [8]$$

where U represents the conserved variables, λ the eigenvalues of the Jacobian matrix and α, β numerical coefficients [Murillo and García-Navarro 2013]. For the temperature transport, a 1D approach following the 2D extension of Morales-Hernández *et al.* (2019) is applied using the conservative form of the transport equation

$$(hT)_i^{n+1} = (hT)_i^n - \frac{\Delta t}{\Delta x}\left[(\mathrm{q}T)_{i-1/2}^{\downarrow} - (\mathrm{q}T)_{i+1/2}^{\downarrow}\right]^n \quad [9]$$

where $q^{\downarrow}$ is the numerical flux at a cell edge, that is computed generally as

$$q_{i+1/2}^{\downarrow} = q_i + \left(\tilde{\lambda}^- \tilde{\gamma} \tilde{\mathbf{e}}\right)_{i+1/2} \quad [10]$$

On the other hand, the temperature is also evaluated at cell edges as $T^{\downarrow}$ defined as

$$T_{i+1/2}^{\downarrow} = \begin{cases} T_i & \text{if } q_{i+1/2}^{\downarrow} > 0 \\ T_{i+1} & \text{if } q_{i+1/2}^{\downarrow} < 0 \end{cases} \quad [11]$$

following Morales-Hernández *et al.* 2019. For both equations, (8) and (9), the time step size, Δt, is restricted by the CFL stability condition due to its explicit character

$$\Delta t = CFL \frac{\Delta x}{max\,\{\lambda\}_i} \quad [12]$$

Note that the time step size is dynamically computed along the simulation and depends on mesh size and wave celerities. The CFL must be between 0 and 1.

Due to the application of the model, the wet/dry fronts must be robustly implemented in order to avoid non-physical solutions of water depths and velocities and to ensure bounded values of temperature. Non-physical solutions may appear when including a transported scalar, such is temperature, as a new conserved variable coupled with the system. Thus, a proper implementation of the approximate Roe solver must be performed allowing accurate and conservative solutions (Murillo *et al.* 2012).

The numerical flux defined in equation (10) must be consequently defined following the fix of the contributions done when the wet-dry algorithm is used to control wet-dry fronts. Therefore, when a wet-dry front is detected and the contributions are reversed following Murillo *et al.* 2012, the numerical flux contributions for the transport equations must be also oriented in the same direction.

3. VALIDATION

3.3 Steady reference solution

To validate the model, two steady flow reference solutions have been computed following Martínez-Aranda *et al.* (2020) whose work is based on MacDonald (1996) tests for one-layer flows. The system of equations is simplified to steady ones removing temporal derivatives and assuming a constant discharge in both layers. By applying this procedure, the system can be re-written as:

$$\frac{d(q_1)}{dx} = 0 \qquad [12]$$

$$\frac{dh_1}{dx}(1 - Fr_1^2) = -\left(\frac{dz_b}{dx} + \frac{dh_2}{dx}\right) - \frac{\tau_w}{gh_1\rho_1} \qquad [14]$$

$$\frac{d(q_2)}{dx} = 0 \qquad [15]$$

$$\frac{dh_2}{dx}(1 - Fr_2^2) = -\left(\frac{dz_b}{dx}\right) + \frac{\tau_w}{gh_2\rho_2} - \frac{\tau_b}{gh_2\rho_2} \qquad [16]$$

that can be easily computed by using an ODE-solver. In this case, the Python function *odeint* from *Scipy* library has been used. The spatial distribution of the upper layer depth and both constant discharges are given as input, while the lower layer depth and bottom are provided as result. Additional values needed to define the solutions are: bottom, $z_b(0)$, and lower, $h_2(0)$, layer boundary conditions (at x=0m), densities and friction parameters. Two different cases without and with friction, terms have been computed: case 3.A and case 3.B, respectively.

3.4 Numerical results

Two steady states are simulated with the two-layer model and compared with the reference solutions described in the former subsection. In Table 1, all the chosen parameters set in the ODE-solver to solve system (12)-(16) are summarized.

Table 1. Parameters to define reference steady solutions.

	RHO1	RHO2	Q1	Q2	$\mathbf{z_b(0)}$	$\mathbf{h_2(0)}$	$\mathbf{C_f}$	$\mathbf{n_b}$
CASE 3.A	1,0	3,0	1,0	0,4	0,5	1,5	0,0	0,0
CASE 3.B	1,0	3,0	1,0	2,0	1,5	0,4	0,01	0,04

The numerical simulations are carried out with a 300 cells mesh and a CFL of 0,95. The constant discharge of the steady solution is set at each layer as inflow boundary condition, while the constant fluid level at the outflow boundary is imposed at outlet condition. Both numerical simulations are carried out starting with an initial condition given by a constant fluid level determined by inlet boundary condition (at x = 0 m). A transitory simulation is developed until the steady state is reached to ensure convergence.

Figure 2 shows the evolution of the simulation 3.A until the steady state is reached. The solid line represents the numerical simulation, while the static dashed line stands for the reference steady solution. At initial time (Figure 2a and 2b), rest condition is set so that velocities are null in the whole channel. At t = 300 s (Figure 2c and 2d), a hydraulic jump is generated while the results converge to the steady state due to the lack of friction and the high velocities. Finally, t = 1000 s, the reference solution is achieved by the model. The analogous results can be seen in Figure 3 for the 3.B case. For this situation, as there is

friction at the bed layer and at the fluids interface, the case presents an asymmetrical profile. Nevertheless, the reference solution for this case is also perfectly achieved at t = 500 s.

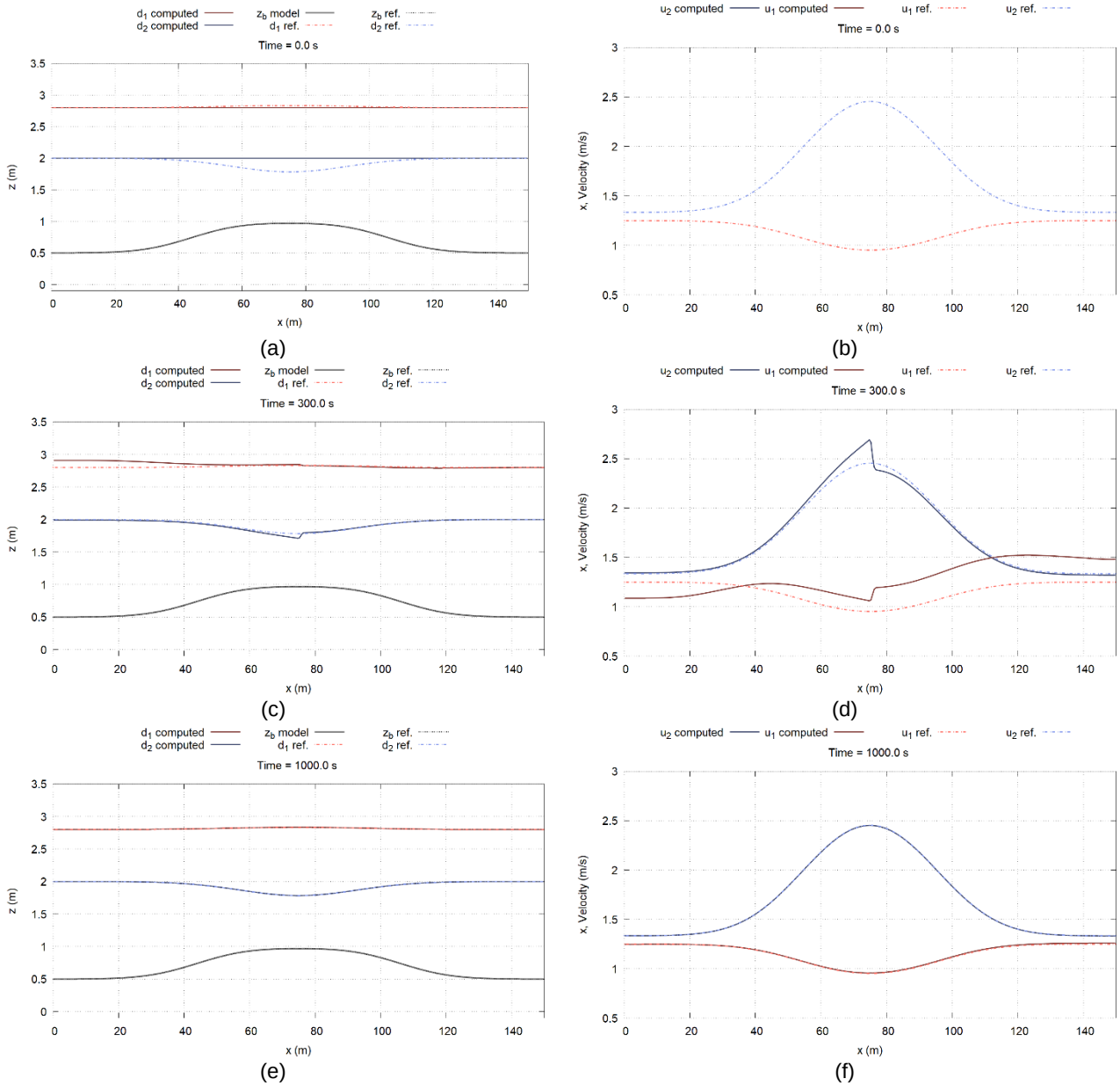

Figure 2. Longitudinal profile of numerical water level (left) and velocities (right) in solid lines compared with the steady reference solution in dashed line for case 3.A at different times.

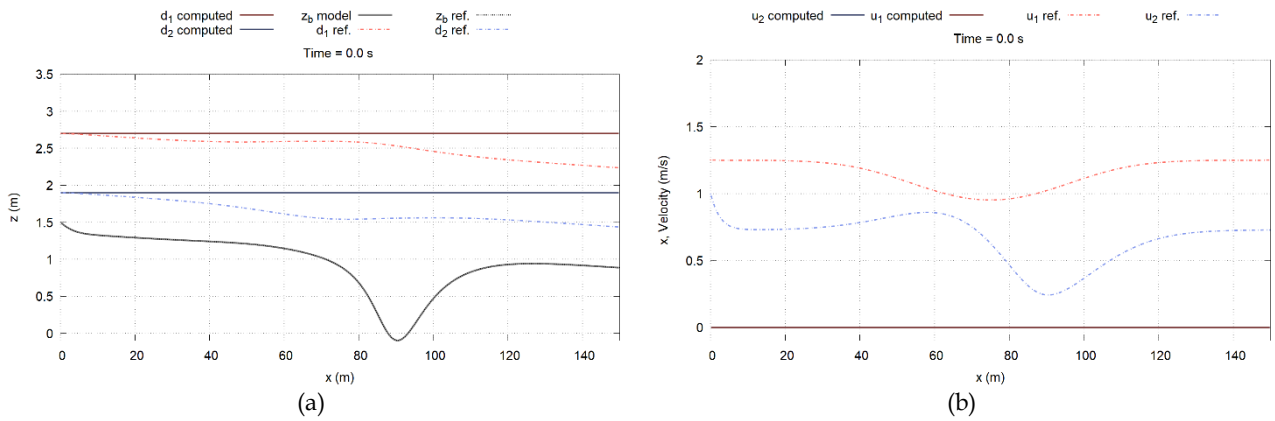

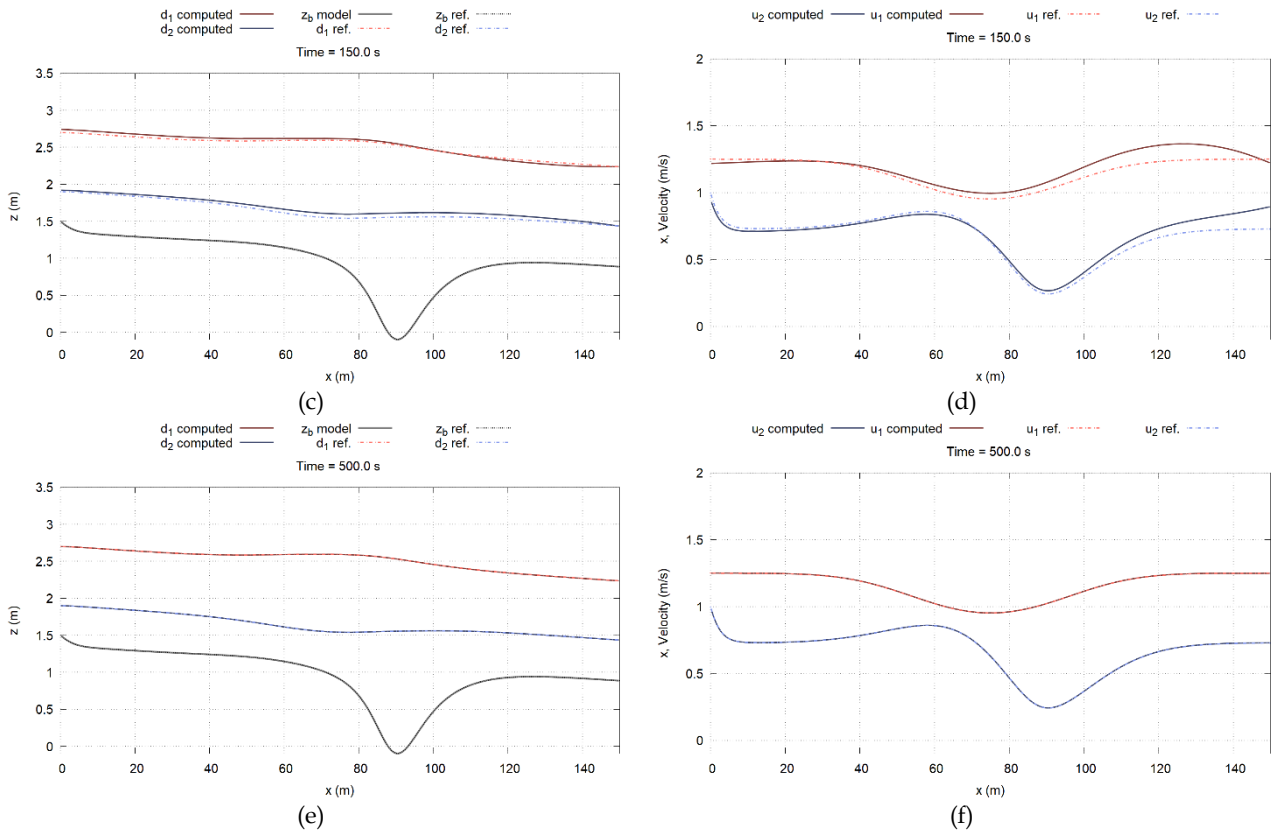

Figure 3. Longitudinal profile of numerical water level (left) and velocities (right) in solid lines compared with the steady reference solution in dashed line for case 3.B at different times.

4. OIL-SPILL SIMULATION

Once the model has been validated, it is applied to a transient test case that represents an oil spill in a coastal water volume. The behavior of the model is tested with wet/dry fronts and under unsteady conditions provoked by coastal-wise waves.

The test case consists of a water volume (ρ_1=1000kg/m^3) initially at rest and two independent initial water columns of oil (ρ_2=800kg/m^3) that spread over the water as the simulation starts, as depicted in Figure 4(a). One of them is initially at T = 300 K while the other is at T = 350 K, as can be seen in Figure 4(b). Additionally, the volume of water has a left boundary condition of variable level that generates inlet waves. This test case is based on a real experimental setup that can be seen in Beji and Battjes (1993), where all the geometric and boundary data are detailed. As a preliminary result, all the heat exchanges have been neglected. The computational mesh is built with 1000 computational cells and the simulation runs for 100 s.

At the first stages, the two oil columns start to spread as seen in Figure 4(c). After a while, a thin slick is created and both spots start to mix, as seen in pictures (e) and (f) of Figure 4. The results show that model behaves logically in wet/dry situations and temperature is transported ensuring mass and energy conservation without any numerical oscillation. And maintaining the initial temperature value at the upper layer wet-dry fronts.

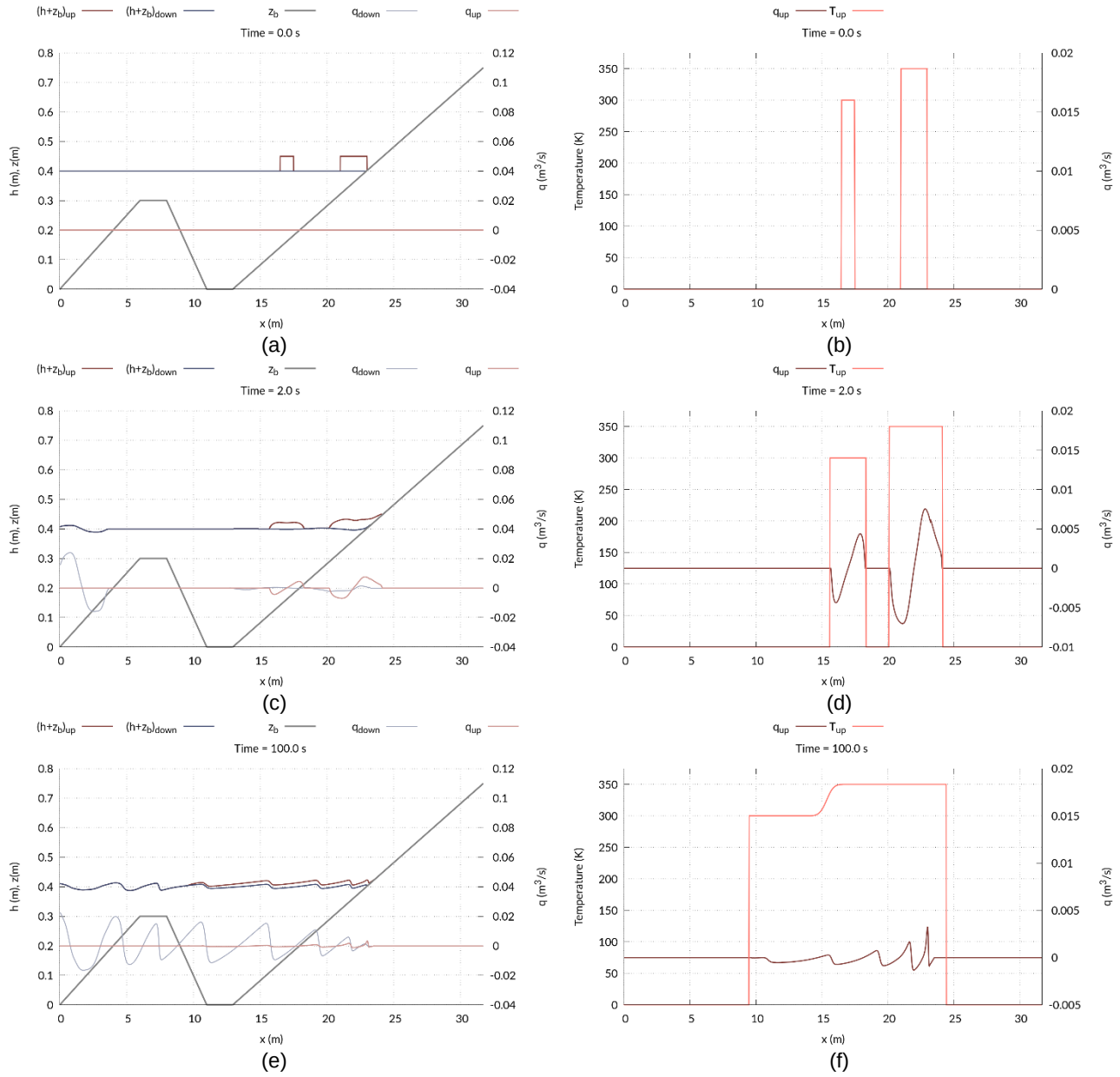

Figure 4. Longitudinal profile of water level, discharge and bottom for oil spill simulation at different times (left) and longitudinal profile of upper layer temperature (right) together with upper discharge.

5. CONCLUSIONS

Oil spills over water volumes can be simulated with two-layer models with the aim of providing to the oil layer its own characteristics and rheological behavior, since traditionally it has been only transported as a passive solute. To do so, a two-layer shallow water type model has been implemented with an additional hypothesis: a null pressure effect from upper oil layer over the huge water volume below. The challenge of those models resides on the numerical stability due to the presence of very low oil depths and wet/dry fronts transporting temperature.

The presented model has been validated through reference solutions for steady states. With and without the presence of friction stresses, no instabilities have been detected and a good agreement has been achieved. Additionally, a hypothetical oil spill has been simulated to ensure the robust behavior of the model in the presence of wet/dry fronts. Good results are presented in terms of stability even for a low slick thickness.

Future research must be done concerning heat exchange, diffusion terms and testing more complex friction laws that could reproduce better the oil performance.

6. ACKNOWLEDGEMENTS

This research was partially funded by the PGC2018-094341-B-I00 research project of the Ministry of Science and Innovation/FEDER. Additionally, Isabel Echeverribar wants to thank to the MINECO for her Industrial Doctorate Research Grant DIN2018-010036.

7. REFERENCES

Beji, S. and Battjes, J. (1993) Experimental investigation of wave propagation over a bar. *Coastal Engineering*, 19 (1-2), 151-162.

Dugdale, S. J. and Hannah, D. M. and Malcolm, I. A. (2017) River temperature modelling: A review of process-based approaches and future directions. *Earth-Science Reviews*, 175, 97-113.

Hoult, D.P. (1972) Oil spreading on the Sea. *Annu. Rev. Fluid Mechanics,* 4, p. 341-268.

MacDonald, I. (1996) Analysis and computation of steady open channel flow. PhD thesis, University of Reading, Reading, UK.

Martínez-Aranda, S. and Ramos-Pérez, A. and García-Navarro, P. (2020) A 1D shallow-flow model for two-layer flows based on FORCE scheme with wet-dry treatment. *Journal of Hydroinformatics*, 22 (5), 1015-1037.

Morales-Hernández, M. and Murillo, J. and García-Navarro, P. (2019) Diffusion-dispersion numerical discretization for solute transport in 2D transient shallow-flows. *Environmental Fluid Mechanics*, 19, 1217-1234.

Murillo, J. and Martínez-Aranda, S. and Navas-Montilla, A. and García-Navarro, P. (2020) Adaptation of flux-based solvers to 2D two-layer shallow flows with variable density including numerical treatment of the loss of hyperbolicity and drying/wetting fronts. *Journal of Hydroinformatics*, 22 (5), 972-1014.

Murillo, J. and García-Navarro, P. (2013) Energy balance numerical schemes for shallow water equations with discontinuous topography. *Journal of Computational Physics*, 236 (1), 119-142.

Murillo, J. and Latorre, B. and Garcia-Navarro, P. (2012) “A Riemann solver for unsteady computation of 2D shallow flows with variable density,” *Journal of Computational Physics*, vol. 231 (14), 4775-4807.

Ripa, P. (1995). On improving a one-layer ocean model with thermodynamics. *Journal of Fluid Mechanics*, 303, 169-201

Spaulding, M. L. (2017) State of art review and future directions in oil spill modeling. *Marine Pollution Bulletin*, 115, p. 7-19.

Tkalich, P. (2006) A CFD solution of oil spill problems. *Environmental Modelling and Software*, 21, 271-282.